ON THE IMPACT OF HEADLAND BYPASSING ON SHORELINE CHANGE IN A ONE-LINE MODEL

Elsa Durand, Vincent Marieu, Bruno Castelle, Deborah Idier, Arthur Robinet, Thomas Guerin

To cite this version:

Elsa Durand, Vincent Marieu, Bruno Castelle, Deborah Idier, Arthur Robinet, et al.. ON THE IMPACT OF HEADLAND BYPASSING ON SHORELINE CHANGE IN A ONE-LINE MODEL. Coastal Sediments 2023, Apr 2023, New Orleans, United States. pp.1364-1371, 10.1142/9789811275135_0126. hal-04265962

ON THE IMPACT OF HEADLAND BYPASSING ON SHORELINE CHANGE IN A ONE-LINE MODEL

ELSA DURAND[1,2,4], VINCENT MARIEU[1], BRUNO CASTELLE[1], DEBORAH IDIER[2], ARTHUR ROBINET[3], THOMAS GUERIN[4]

1. *Univ. Bordeaux, CNRS, Bordeaux INP, EPOC, UMR 5805, Pessac, France.* *elsa.durand@u-bordeaux.fr ; bruno.castelle@u-bordeaux.fr ; vincent.marieu@u-bordeaux.fr*
2. *BRGM, 3 Avenue Guillemin, Orléans, France. d.idier@brgm.fr*
3. *BRGM, 24 Avenue Léonard de Vinci, Pessac, France. a.robinet@brgm.fr*
4. *BW-CGC (Benoit Waeles – Consultant Génie Côtier), Brest, France. thomas.guerin@bw-cgc.fr*

Abstract: The knowledge of future long-term sandy shoreline evolution is necessary for sustainable coastline management. However, the impact of sediment transport due to headland sand bypassing is not yet well addressed in shoreline models. This work aims at implementing a parametric expression for sand bypassing in the reduced complexity shoreline model LX-Shore. The parametrization of the wave-forced sediment bypassing around an isolated headland developed by McCarroll et al. (2021) is implemented. Considering an idealized configuration of a 300-m long, initially straight, sandy coast with a rectangular headland, results show that headland sand bypassing has a substantial impact on the downdrift (updrift) erosion (accretion) pattern and magnitude. Our simulations imply that taking into account bypass transport in long-term shoreline models such as LX-Shore could provide new insights into coastal embayment changes.

Introduction

In a context of significant demographic growth and expected increase in beach erosion and shoreline retreat (Vousdoukas et al., 2020), it is critical to better understand and predict sandy coasts evolution in order to provide sustainable coastal management. Over the last few years, reduced-complexity models such as LX-Shore (Robinet et al., 2018) or CoSMoS-COAST (Vitousek et al., 2017) have been developed to predict long-term (years-decades) shoreline evolution of wave-dominated sandy coasts with low computing times. Nevertheless, the impact of sand bypassing, defined here as sediment transport around natural headlands or anthropogenic groins, has been scarcely addressed using shoreline models. According to Goodwin et al. (2013), this phenomenon greatly influences the evolution of sandy coastlines at large time scales. It can create sand spits at the tip of the obstacles or contributing to the rotation of embayed beaches, which represent 50% of global coasts (King et al., 2021). Recently, improved and generic sediment bypassing parametrizations have been proposed (King et al., 2021; McCarroll et al., 2021), which are compatible with the reduced-complexity shoreline modelling framework.

LX-Shore (Robinet et al., 2018) is a one-line shoreline model which showed good hindcasting and predictive skills for many types of wave-dominated sandy coasts (Robinet et al., 2020; Montaño et al., 2020). However, so far it did not accurately reproduce the effects of sediment transport around headlands, which was only active when the shoreline reached the tip of the obstacle (Castelle et al., 2020). In the present contribution, the parametrization developed by McCarroll et al. (2021) is implemented in LX-Shore, and the effects of headland sand bypassing on shoreline dynamics updrift and downdrift of the structure are addressed considering an idealized configuration of a straight beach with a rectangular headland.

Methods

The LX-Shore model

LX-Shore is a two-dimensional planview cellular-based model. It allows to simulate sandy shoreline evolution on time scales ranging from hours to decades with reasonable computing times (Fig. 1.a, Robinet et al., 2018). The model can be used for many sandy shorelines geometries (e.g. sand spits, islands) and can handle the presence of non-erodible areas (Fig. 1.a). LX-Shore is based on a one-line approach which considers sediment transports due to both longshore and cross-shore processes (Fig. 1.b).

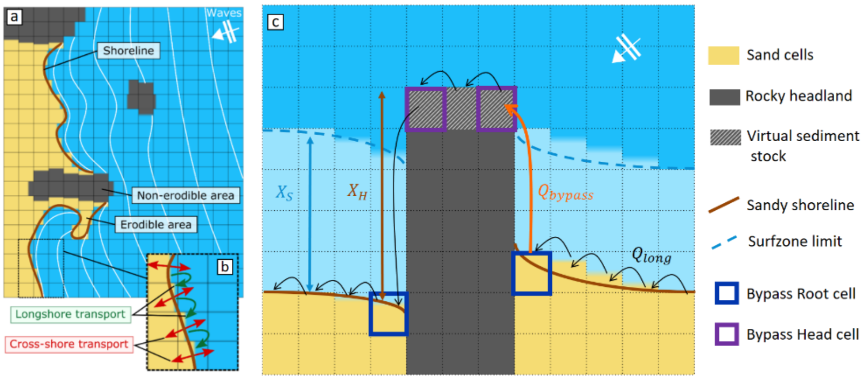

Fig. 1. Overview of the LX-Shore features showing (a) a schematic planview of the model structure and processes at work with (b) locations where longshore and cross-shore transports are calculated (adapted from Robinet et al., 2018). (c) Schematic representation of the numerical implementation of bypass transport around a rectangular rocky headland

In this study, cross-shore sediment transport is switched off in order to focus on longshore transport and the effects of headland sand bypassing, while longshore sediment flux (Q_{long}) is computed at the interface of the cells through the Kamphuis (1991) formula. Sediment fluxes are translated in terms of variation of a sediment fraction F, ranging from 0 for water cells to 1 for sandy cells, calculated in a grid composed of squared cells. At each time step, the shoreline position is computed, based on this updated fraction F.

Implementation of the bypass parametrization in LX-Shore

McCarroll et al. (2021) show that the wave-forced sediment bypassing around an isolated headland is mainly controlled by the ratio between headland cross-shore extent X_H and surf zone width X_S, taken as distances from the shoreline next to the headland (Fig. 1.c). Bypassing sediment flux Q_{bypass} (m^3/s) is then approximated as a function of Q_{long} and X_H/X_S:

$$Q_{bypass} = sign(A)p_1A^2 + p_2A, \tag{1}$$

with

$$A = Q_{long}e^{-b_1\left(\frac{X_H}{X_S}\right)^{b_2}} \tag{2}$$

where p_1, p_2, b_1 and b_2 are coefficients adjusted by calibration.

This parametric expression only applies if $0.5 < X_H/X_S < 3$.
Indeed, if $X_H/X_S < 0.5$, i.e. when the obstacle is smaller than half the surf zone, it is assumed that the headland doesn't affect the longshore sand transport and $Q_{bypass} = Q_{long}$.
On the contrary, if $Q_{bypass} < 10^{-4}$ m^3/s, which likely occurs when $X_H/X_S > 3$ and/or during low energy conditions or for nearshore normal waves, it is assumed that the longshore sand transport is blocked by the headland and $Q_{bypass} = 0$.

This parametrization has been implemented in LX-Shore considering an idealized configuration with a rectangular headland (Fig. 1.c). The rocky cells are identified differently depending on whether they are on the sides or on the top of the headland. When the last sandy shoreline cell before a side cell of the obstacle is encountered, it is defined as a *root cell*, i.e. the sandy cell from where the sand bypasses the headland (Fig. 1.c). The sediment flux leaving this cell is then calculated with Q_{bypass}, and the sand is sent to a virtual sediment stock located in the associated *head cell* at the top of the rocky headland. Using the alongshore transport rate Q_{long}, this sand transits alongshore as a virtual stock in the top cells of the headland, and is finally transferred to the other side of the obstacle.

Simulation set-up

The model set-up consists of a 300-m long straight beach interrupted by a rectangular rocky headland (Fig. 2.a). The simulations presented here were performed over a 10-day period, with a 2-hour constant time step and a grid cell size of 10 m. Periodic lateral boundary conditions were implemented, i.e. the sediment fraction leaving the simulation domain from the left boundary re-enters the domain from the right, and vice-versa. The water depth h along the cross-shore axis was retrieved at each time step using an equilibrium Dean profile (Dean, 1991) given by $h=ad^b$ where d is the distance offshore from the shoreline, a = 0.25 and b = 0.67 for the sandy profile, and a = 0.2 and b = 1 for the rocky profile. The depth of closure D_C was set arbitrarily to 5 m. Offshore waves used in the simulation were characterized by a significant wave height H_S of 0.8 m, a peak wave period T_P of 8 s and a random peak angle of incidence θ_P normally distributed around 35° with a standard deviation of 5°. Breaking wave parameters were then computed along the coast with the direct formula of Larson et al. (2010) combined with a shadowing procedure so that waves are not computed and no sediment is transported in areas protected from waves by the headland (shadowed).

Results

Figure 2 shows the results of the two simulations performed with the identical wave conditions described above, with bypass transport module switched on (Fig. 2.c) and switched off (Fig. 2.b).

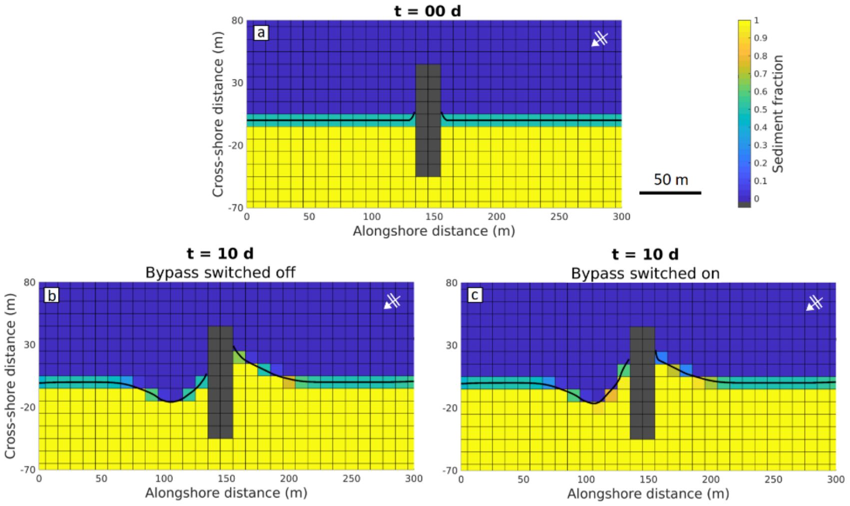

Fig. 2. Results of LX-Shore simulations. (a) Initial shoreline at t=0. (b) 10-days simulation without sediment bypassing. (c) Same simulation with the new implementation of the bypass parametrization in LX-Shore

For a 10-day simulation, the sediment bypass implementation in LX-Shore results in a less pronounced accretion updrift, and a less important erosion downdrift.

Figure 3 shows timestacks of the cross-shore shoreline position with the bypass switched on (Fig. 3.b) and switched off (Fig. 3.a). Both panels show longshore extension of the headland influence of about 50 m after 10 days, for changes in shoreline positions of about tens of meters (accretion updrift, erosion downdrift). The maximum evolution updrift is located along the headland (last cell before the headland), while the maximum evolution downdrift is located a bit further (few cells downdrift of the headland). Finally, when sediment bypass is switched on (panel b), there is a thin area located directly downdrift of the headland where accretion occurs: this illustrates the effect of bypassing which allows sediment to go downdrift of the obstacle. When bypass is switched off (panel a), the shoreline is stable in this area. This is due to the combination of wave obliquity and the use of a parametric shadowing formula resulting in rare occurrences and/or low values of outgoing longshore sediment transport.

To better quantify the impact of sediment bypass, the timestack of the differences between the cross-shore shoreline positions of the two simulations is analyzed (Fig. 3.c). First, the longshore area of influence of activating the sediment bypass reaches about 50 m from the headland updrift and 20 m downdrift. To estimate this area of influence, a shoreline position difference threshold of 0.5 m was considered. Second, the effect on the shoreline position itself is such that after only 10 days of reasonably low-energy obliquely incident waves, erosion (accretion) downdrift (updrift) is reduced by nearly 12 (6) m.

Figure 3.c also shows that the effect of switching on the sediment bypass is not linear in time: it has no impact during the first day, while there is a rapid increase in the differences during the next 3 days, and finally it seems to reach a stabilization phase near 10 days. This soft temporal evolution (little variability) suggests a balance over the time between (1) decreasing longshore sand transport potential due to updrift clockwise shoreline rotation and (2) increasing degree of sand bypassing due to progressively decreasing X_H/X_S.

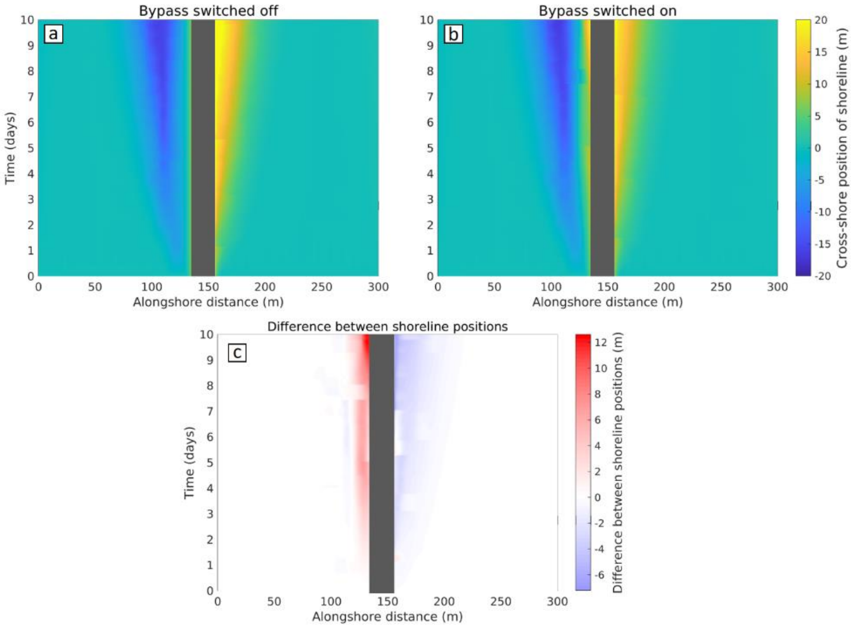

Fig. 3. Timestacks of cross-shore shoreline position (a) when bypass is switched off, (b) when bypass is switched on. (c) Timestack of the difference between shoreline positions (modelled shoreline when bypass switched on minus modelled shoreline when bypass switched off)

Conclusion

A parametric expression of wave-forced sediment bypassing was implemented in a reduced-complexity shoreline model, LX-Shore. Results on an academic case show that headland sand bypassing can have a substantial impact on the erosion/accretion patterns close to the headland. We anticipate that taking into account obstacle sand bypassing in long-term shoreline evolution models such as LX-Shore will improve our understanding of sandy coastline response, including mean embayment planshape and rotation signal of embayed beaches. Further analyses will focus on applying this new version of LX-Shore on embayed beaches and studying the spatio-temporal modes of shoreline variability in presence of sediment bypassing.

Acknowledgements

This work was funded in the scope of an ANRT/CIFRE contract (n°2021/0579) between BW-CGC, Bordeaux University and BRGM, and was performed in the frame of the SHORMOSAT ANR project (grant n° ANR-21-CE01-0015).

References

Castelle, B., Robinet, A., Idier, D., & D'Anna, M. (2020). Modelling of embayed beach equilibrium planform and rotation signal. *Geomorphology*, 369, 107367.

Dean, R.G. (1991). Equilibrium beach profiles: characteristics and applications. *J. Coast. Res*. 7, 53–84.

Goodwin, I. D., Freeman, R., & Blackmore, K. (2013). An insight into headland sand bypassing and wave climate variability from shoreface bathymetric change at Byron Bay, New South Wales, Australia. *Marine Geology*, 341, 29-45.

Kamphuis, J. W. (1991). Alongshore Sediment Transport Rate. Journal of Waterway, Port, *Coastal, and Ocean Engineering*, 117(6), 624-640.

King, E. V., Conley, D. C., Masselink, G., Leonardi, N., McCarroll, R. J., Scott, T., & Valiente, N. G. (2021). Wave, Tide and Topographical Controls on Headland Sand Bypassing. *Journal of Geophysical Research*: Oceans, 126(8).

Larson, M., Hoan, L. X., & Hanson, H. (2010). Direct formula to compute wave height and angle at incipient breaking. *Journal of Waterway port, Coastal and Ocean engineering*, 136(2), 119-122

McCarroll, R. J., Masselink, G., Valiente, N. G., King, E. V., Scott, T., Stokes, C., & Wiggins, M. (2021). An XBeach derived parametric expression for headland bypassing. *Coastal Engineering*, 165, 103860.

Montaño, J., Coco, G., Antolínez, J.A.A. et al. (2020). Blind testing of shoreline evolution models. *Scientific Reports* 10, 2137

Robinet, A., Idier, D., Castelle, B., & Marieu, V. (2018). A reduced-complexity shoreline change model combining longshore and cross-shore processes: The LX-Shore model. *Environmental Modelling & Software*, 109, 1-16.

Robinet, A., Idier, D., Le Cozannet, G., Castelle, B. (2018). Simulating sea-level rise impacts on shoreline change along a wave-dominated sandy coast with the LX-Shore model. 10.13140/RG.2.2.21487.28329.

Robinet, A, Castelle, B, Idier, D, Harley, M.D., Splinter, K.D. (2020). Controls of local geology and cross-shore/longshore processes on embayed beach shoreline variability, *Marine Geology*, Volume 422

Vitousek, S., Barnard, P.L., Limber, P., Erikson, L., Cole, B. (2017). A model integrating longshore and cross-shore processes for predicting long-term shoreline response to climate change, *J. Geophys. Res. Earth Surf*., 122, 782–806

Vousdoukas, M.I., Ranasinghe, R., Mentaschi, L. et al. (2020). Sandy coastlines under threat of erosion. *Nat. Clim. Chang*. 10, 260–263